



Universiteit
Leiden
The Netherlands

Solvent tolerance mechanisms in *Pseudomonas putida*

Kusumawardhani, H.

Citation

Kusumawardhani, H. (2021, March 11). *Solvent tolerance mechanisms in Pseudomonas putida*. Retrieved from <https://hdl.handle.net/1887/3151637>

Version: Publisher's Version

License: [Licence agreement concerning inclusion of doctoral thesis in the Institutional Repository of the University of Leiden](#)

Downloaded from: <https://hdl.handle.net/1887/3151637>

Note: To cite this publication please use the final published version (if applicable).

Cover Page



Universiteit Leiden



The handle <https://hdl.handle.net/1887/3151637> holds various files of this Leiden University dissertation.

Author: Kusumawardhani, H.

Title: Solvent tolerance mechanisms in *Pseudomonas putida*

Issue Date: 2021-03-11

CHAPTER 3

Comparative analysis reveals the modular functional build-up of megaplasmid pTTS12 of *Pseudomonas putida* S12: a paradigm for transferable traits, plasmid stability and inheritance?

Hadiastri Kusumawardhani†, Rohola Hosseini†, Johannes H. de Winde

†H. K. and R. H. contributed equally to this work.

Submitted for publication.

DOI: 10.1101/2020.06.19.162511

Abstract

The *Pseudomonas putida* S12 genome contains 583 kbp megaplasmid pTTS12 that carries over 600 genes enabling tolerance to various stress conditions, including the solvent extrusion pump SrpABC. We performed a comparative analysis of pTTS12 against 28915 plasmids from NCBI databases. We investigated putative roles of genes encoded on pTTS12 and further elaborated on its role in the establishment and maintenance of several stress conditions, specifically focusing on solvent tolerance in *P. putida* strains. The backbone of pTTS12 was found to be closely related to that of the carbapenem-resistance plasmid pOZ176, member of the IncP-2 incompatibility group, although remarkably the carbapenem resistance cassette is absent from pTTS12. Megaplasmid pTTS12 contains multiple transposon-flanked cassettes mediating resistance to various heavy metals such as tellurite, chromate (Tn7), and mercury (Tn5053 and Tn5563). Additionally, pTTS12 also contains a P-type, Type IV secretion system (T4SS) supporting self-transfer to other *P. putida* strains. This study increases our understanding in the build-up of IncP-2 plasmids and several promising exchangeable gene clusters to construct robust microbial hosts for biotechnology applications.

Importance

Originating from various environmental niches, large numbers of bacterial plasmids have been found carrying heavy metal and antibiotic resistance genes, degradation pathways and specific transporters for organic solvents or aromatic compounds. Such genes may constitute promising candidates for novel synthetic biology applications. Our systematic analysis of gene clusters encoded on megaplasmid pTTS12 underscores that a large portion of its genes is involved in stress response increasing survival under harsh conditions like heavy metal and organic solvent resistance. We show that pTTS12 belongs to the IncP-2 plasmid family. Comparative analysis of pTTS12 provides thorough insight into the structural and functional build-up of members of the IncP-2 plasmid family. pTTS12 is highly stable and carries a complex arrangement of transposable elements containing heavy metal resistance clusters as well as distinct aromatic degradation pathways and solvent-extrusion pump. This offers interesting insight into the evolution of solvent tolerance in the *P. putida* family.

Introduction

Megaplasmids as transferable vehicles of environmental resistance genes

Bacteria may use plasmids as autonomous, self-replicating elements driving horizontal transfer of genes (HGT) that confer resistance to otherwise detrimental conditions. As such, these extrachromosomal entities often confer advantageous characteristics for the host strain (1–3). The rapid spread of resistance genes through these, usually large conjugative plasmids is further facilitated by the presence of a variety of mobile genetic elements such as transposons, integrons and insertion sequences (IS's) (4–7). The spread of multidrug resistance (MDR) via mobile genetic elements has been the subject of investigation for a number of years (8). Despite those efforts, the role and functioning of megaplasmids is still poorly understood. Recent studies highlighted the role of megaplasmids in the spread of MDR in the opportunistic pathogen *Pseudomonas aeruginosa* (1, 2). Strains of its close relative, *Pseudomonas putida*, have been known to harbor large conjugational plasmids, conferring resistance to environmental threats (3, 9). Plasmids of the *Pseudomonas* family are classified by incompatibility groups, that exhibit various modes of compatibility and transferability (10). We have chosen to study the recently identified megaplasmid pTTS12 of *Pseudomonas putida* S12 in comparison with a number of other large plasmids of the *Pseudomonas* family, in order to elucidate key elements governing HGT, stability and essential functions.

Solvent tolerance in *Pseudomonas putida* S12; resistance as a benefit for biotechnology

Pseudomonas putida S12 is a gram-negative soil bacterium which was isolated on styrene as a sole carbon source (11). This strain shows a remarkable tolerance towards non-metabolized organic solvents (e.g. toluene) (12). Such high tolerance towards organic solvents presents a beneficial trait and advantage for bioproduction of aromatics and biofuel (13, 14). Due to its solvent tolerance and versatile metabolism, *P. putida* S12 excels as a microbial host for production of valuable chemicals (15–19). Removal of organic solvent molecules from the bacterial cell membrane is essential and carried out by SrpABC, a resistance-nodulation-cell division (RND) family efflux pump (12, 20). Membrane compaction and the upregulation of chaperones, general stress responses, and TCA cycle-related enzymes support a further in-

trinsic solvent tolerance in *P. putida* S12 (21–24).

We recently found through whole-genome sequencing that the genome of *P. putida* S12 consists of a 5.8 Mbp chromosome and a 583 kbp single-copy megaplasmid pTTS12 (25). Interestingly, both the SrpABC RND-efflux pump and the styrene degradation pathway which are major distinctive features of *P. putida* S12, are encoded on this megaplasmid. The genome of *P. putida* S12 contains a large number of several types of mobile elements, spread over both chromosome and megaplasmid pTTS12 (25–27). Some of these insertion sequences were shown to be involved in the regulation and adaptation towards stress conditions, for example during the solvent stress (4, 28). Like *P. putida* S12, related solvent-tolerant *P. putida* DOT-T1E and *Pseudomonas taiwanensis* VLB120 have been shown to harbor megaplasmids of 121 kb and 312 kb, respectively (29, 30). Indeed, those plasmids encode RND-type efflux pumps and biodegradative pathways for aromatic compounds, similar to *P. putida* S12. To further characterize pTTS12, we here performed a comparative analysis against a large number of other megaplasmids from Refseq and Nuccore databases. With this analysis, we aimed at identifying the origin of the pTTS12 plasmid and understanding the build-up of environmental-stress related gene clusters in pTTS12.

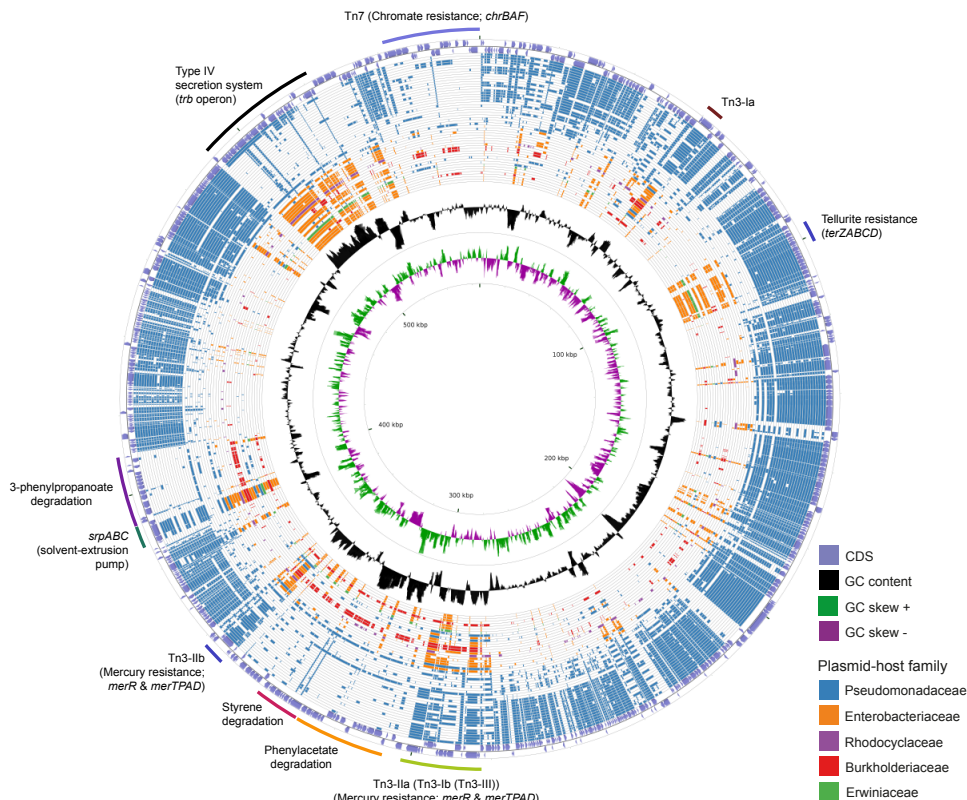
Results

Comparative analysis of megaplasmid pTTS12

The 583 Kbps megaplasmid pTTS12 (GenBank accession no. CP009975) is a single-copy plasmid encoded in *P. putida* S12 (25). For this paper, annotations for pTTS12 were further extended and the overall sequence was corrected based on our previous observations of an additional seven ISS12 mobile elements (4). pTTS12 encodes 609 genes of which 583 are single copy and 15 genes are duplicated at least once. These genes were divided into 232 putative operons for subsequent ordered genes in forward or reverse strand with less than 20 bps distance. The operons were clustered together based on the function of genes encoded within these clusters.

Comparative analysis was performed with 28915 plasmids larger than 2 kb in length, acquired from the Refseq database (<https://www.ncbi.nlm.nih.gov/refseq/>) combined with additional sequences from the Nuccore database (<https://www.ncbi.nlm.nih.gov/nuccore/>). The top 50 plasmids encoding homologues of pTTS12 proteins are visualized in a circular plot using CGView (31) as shown on Fig. 3.1, and listed in Table 3.1. In Fig. 3.1, the outer purple

line represents pTTS12 with forward coding genes on top of the line and the reverse coding gene sequences below the line. Each of the subsequent 50 inner circles represents a single plasmid and is colored based on the family of its host. In case no homologous protein was identified for a pTTS12 counterpart, that space on the circle was left blank. The extended circular plot of the top 500 plasmids encoding homologues of pTTS12 can be found in Fig. 3.S1.



pTTS12 coding sequences (CDS) were aligned to 28915 other plasmids available at NCBI Refseq and Nuccore databases. The outer light purple ring represents the CDS of plus and minus strand of pTTS12. In the inner ring, the GC content is represented in black and the positive and negative GC skew are represented in green and purple respectively. The plasmids are ordered based on their similarity and coverage to pTTS12 CDS from outermost to innermost of the plot with each ring representing a single plasmid as listed in Table 3.1. Ring colors represent different plasmid-host families; Pseudomonadaceae (blue), Enterobacteriaceae (orange), Rhodocyclaceae (purple), Burkholderiaceae (red), and Erwiniaceae (green). The position of the gene clusters of interest are annotated in the figure. An extended circular plot of the top 500 plasmids with highest identity scores to pTTS12 are shown in Fig. 3.S1.

The majority of plasmids highly similar to pTTS12 were found in *Pseudomonas* type strains (Table 3.1). The relative identity scores presented in Table 3.1 were calculated as a percentage of total scores of each plasmid divided by the total identity score obtained for pTTS12 itself. The plasmid most similar to pTTS12 is pOZ176 from *P. aeruginosa* PA96 which was previously categorized as a member of incompatibility group P-2 (IncP-2). pOZ176 and pTTS12 share no less than 71% similarity of their encoded genes indicating that these plasmids share a similar IncP-2 backbone. However, while pOZ176 encodes a carbapenem-resistance gene cluster typical for several pathogenic *P. aeruginosa* strains (2), pTTS12 of *P. putida* S12 does not share this feature.

Table 3.1. List of 50 plasmids with the highest similarity scores to pTTS12. pTTS12 coding sequences (CDS) were aligned to other megaplasmids available at NCBI databases. The relative similarity score was calculated by dividing total scores for each plasmid by total score obtained for pTTS12 itself.

Rank	Strain	Plasmid	Taxid	Length (bp)	Relative similarity
	<i>Pseudomonas putida</i> S12	pTTS12	1215087	583900	100.00%
1	<i>Pseudomonas aeruginosa</i> PA96	pOZ176	145792	500839	72.54%
2	<i>Pseudomonas aeruginosa</i> strain FFUP_PS_37	pJB37	287	464804	69.30%
3	<i>Pseudomonas aeruginosa</i> strain AR_0356	unnamed2	287	438531	67.97%
4	<i>Pseudomonas aeruginosa</i> strain AR441	unnamed3	287	438529	66.23%
5	<i>Pseudomonas putida</i> strain SY153	pSY153-MDR	303	468170	64.70%
6	<i>Pseudomonas aeruginosa</i> strain T2436	pBT2436	287	422811	64.69%
7	<i>Pseudomonas koreensis</i> strain P19E3	p1	198620	467568	64.44%
8	<i>Pseudomonas putida</i> strain 12969	p12969-DIM	303	409102	64.43%
9	<i>Pseudomonas aeruginosa</i> strain T2101	pBT2101	287	439744	64.43%
10	<i>Pseudomonas aeruginosa</i> strain PA298	pBM908	287	395774	63.99%
11	<i>Pseudomonas aeruginosa</i> isolate RW109	RW109	287	555265	63.75%
12	<i>Pseudomonas aeruginosa</i> strain PA121617	pBM413	287	423017	63.20%
13	<i>Pseudomonas aeruginosa</i> strain PABL048	pPABL048	287	414954	62.82%
14	<i>Pseudomonas aeruginosa</i>	p727-IMP	287	430173	62.75%
15	<i>Pseudomonas aeruginosa</i> strain AR439	unnamed2	287	437392	62.00%
16	<i>Pseudomonas citronellolis</i> strain SJTE-3	pRBL16	53408	370338	61.12%
17	<i>Pseudomonas aeruginosa</i>	p12939-PER	287	496436	60.86%
18	<i>Pseudomonas aeruginosa</i>	pA681-IMP	287	397519	59.50%
19	<i>Pseudomonas aeruginosa</i>	pR31014-IMP	287	374000	55.58%

Rank	Strain	Plasmid	Taxid	Length (bp)	Relative similarity
20	<i>Pseudomonas taiwanensis</i> VLB120	pSTY	69328	321653	21.65%
21	<i>Pseudomonas fluorescens</i> SBW25	pQBR103	216595	425094	20.48%
22	<i>Pseudomonas syringae</i> pv. <i>maculicola</i> str. ES4326	pPma4326F	629265	387260	20.16%
23	<i>Pseudomonas putida</i> strain KF715	pKF715A	303	483376	16.63%
24	<i>Pseudomonas stutzeri</i> strain YC-YH1	pYCY1	316	225945	16.06%
25	<i>Pseudomonas fluorescens</i> SBW25	pQBR57	216595	307330	14.45%
26	<i>Pseudomonas aeruginosa</i> strain PA83	unnamed1	287	398087	14.42%
27	<i>Pseudomonas aeruginosa</i> strain DN1	unnamed1	287	317349	14.24%
28	<i>Pseudomonas monteili</i> strain FDAAR-GOS_171	unnamed	76759	60588	13.85%
29	<i>Salmonella enterica</i> strain 8025	p8025	28901	311280	11.99%
30	<i>Pseudomonas luteola</i> strain FDAAR-GOS_637	unnamed1	47886	585976	10.92%
31	<i>Enterobacter hormaechei</i> subsp. <i>steigerwaltii</i> strain 34998	p34998	299766	239973	10.39%
32	<i>Enterobacter hormaechei</i> strain A1	pln-cHI2-1502264	158836	309444	10.37%
33	<i>Leclercia adecarboxylata</i> strain Lec-476	pLec-476	83655	311758	10.06%
34	<i>Enterobacter hormaechei</i> subsp. <i>hoffmannii</i> strain AR_0365	unnamed1	1812934	328871	9.98%
35	<i>Azospira</i> sp. I09	pAZI09	1765049	397391	9.98%
36	<i>Citrobacter freundii</i> strain SL151	unnamed1	546	229406	9.89%
37	<i>Cupriavidus metallidurans</i> strain FDAAR-GOS_675	unnamed3	119219	2586495	9.54%
38	<i>Cupriavidus metallidurans</i> CH34	megaplasmid	266264	2580084	9.53%
39	<i>Enterobacter hormaechei</i> subsp. <i>hormaechei</i> strain 34983	p34983	301105	328905	9.41%
40	<i>Escherichia coli</i> strain CFSAN064035	pGMI17-003_1	562	310064	9.19%
41	<i>Pseudomonas</i> sp. XWY-1	pXWY	2069256	394537	9.15%
42	<i>Klebsiella oxytoca</i> strain CAV1374	pKPC_CAV1374	571	332956	9.12%
43	<i>Pseudomonas veronii</i> 1YdBTEX2	pPVE	1295141	373858	9.06%
44	<i>Pantoea</i> sp. PSNIH2	pPSP-75c	1484157	378808	9.04%
45	<i>Klebsiella michiganensis</i> strain AR375	unnamed2	1134687	340462	8.96%
46	<i>Citrobacter freundii</i> complex sp. CFNIH9	pCFR-eb27	2077149	355789	8.82%
47	<i>Ralstonia solanacearum</i> strain HA4-1	HA4-1MP	305	1947245	8.82%
48	<i>Enterobacteriaceae bacterium</i> ENNIH1	pENT-1f0b	2066051	302640	8.78%
49	<i>Leclercia</i> sp. LSNIH1	pLEC-1cb1	1920114	341250	8.74%
50	<i>Leclercia</i> sp. LSNIH3	pLEC-7c0d	1920116	330021	8.74%

Surprisingly, pTTS12 shares only 21% of sequence similarity with the pSTY plasmid of *P. taiwanensis* VLB120. The major and only gene clusters shared between pTTS12 and pSTY are involved in styrene degradation, phenylpropionic acid degradation, and solvent efflux pump (SrpABC). Interestingly, the genes shared between pTTS12 and pSTY are absent in all other *Pseudomonas* plasmids, except for the solvent efflux pump gene cluster which is similar with TtgGHI efflux pump from the pGRT-1 plasmid of *P. putida* DOT-T1E. The regions encoding solvent efflux pump and phenylpropionic acid degradation are clustered together and have identical synteny in pTTS12 and pSTY (Fig. 3.S2). However, the plasmids do not share any mobile genetic elements surrounding this cluster that might indicate a mechanism of acquisition or transfer. The similarity of the styrene degradation clusters and solvent efflux pump - phenylpropionic acid degradation clusters between pTTS12 and pSTY were 99% and 80%, respectively.

Between 8% to 12% of encoded proteins from pTTS12 can also be found in other genera than *Pseudomonas* (Table 3.1). Several plasmids from *Salmonella*, *Enterobacter*, *Citrobacter*, *Leclersia*, *Klebsiella*, *Pantoea*, *Polaromonas*, and *Cupriavidus* species shared homologous proteins involved in the T4SS conjugation, replication machinery, and plasmid maintenance. Like other IncP-2 plasmids, pTTS12 contains multiple transposable elements, particularly Tn3 mobile elements (Fig. 3.1). This mobile element encodes for heavy metal resistance genes that are predominantly present in IncP-2 plasmids. Additionally, pTTS12 carries a unique Tn7-element consisting of several chromate resistance genes.

Distinctive conjugation machinery of pTTS12

Megaplasmid pTTS12 contains a P-type T4SS (Type IV secretion system) conjugation system (RPPX_28670-RPPX_28725), sharing synteny with the prototype *trb* operon from *A. tumefaciens* pTiC58 (Fig. 3.2A). For an operational T4SS conjugation machinery, a T4SS gene cluster, type IV coupling protein (T4CP) and a relaxase protein are required (32). An additional *traG* (RPPX_28650), which may serve as a T4CP, is located upstream of the T4SS cluster. Further upstream of the T4SS and T4CP, a putative virD2-like gene (RPPX_28750) and an operon consisting of *parB*, *parA* and *repA* (RPPX_28765-28775) are encoded on pTTS12. The putative virD2-like gene (RPPX_28750) may play a role as a relaxase which is important for the transferability of pTTS12.

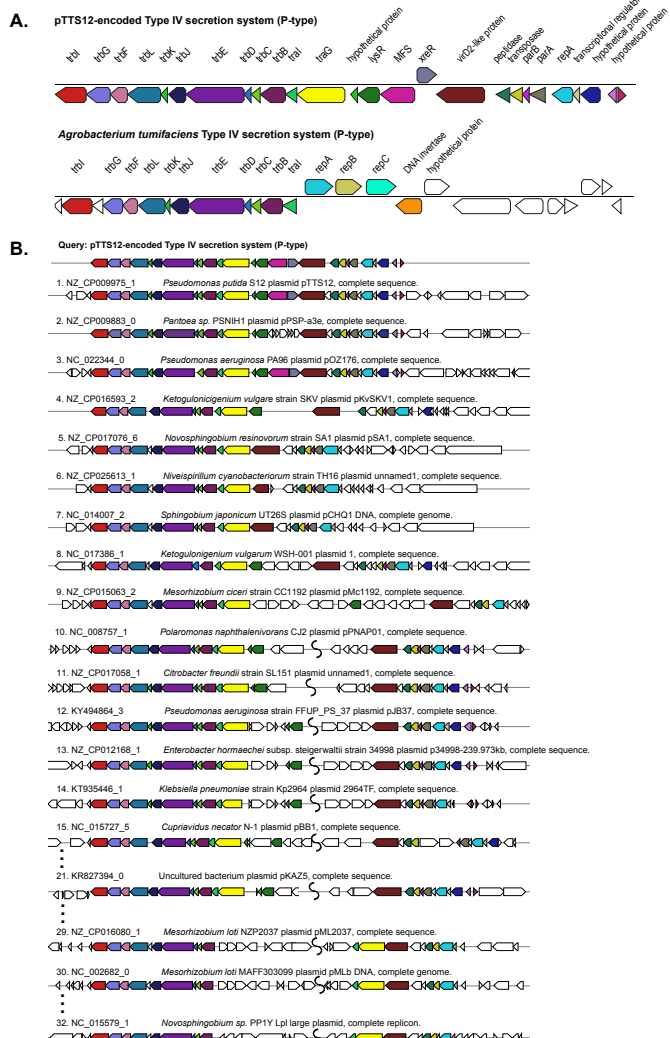


Fig. 3.2. Structure and synteny of pTTS12 conjugation system

A. The arrangement of the T4SS gene cluster found in pTTS12 and the prototype *trb* operon from *Agrobacterium tumefaciens* (pTiC58). The colors represent different genes in the cluster and same colors are assigned for the homologous genes. The gene names are indicated above the respective clusters. pTTS12/T4SS and the *trb* operon of pTiC58 share synteny for 11 genes (*tbl* to *trb*), while other parts are clearly different.

B. Synteny plot of the T4SS gene cluster of pTTS12 for plasmid conjugation, replication and partitioning compared with other plasmids. This visualization was generated using multigeneblast software (49). The numbers refer to the order of decreasing synteny. For the sake of clarity, several plots were removed from this figure, indicated by the dots. The colors represent different genes in the cluster corresponding to color-coding in panel A. Putative coupling-protein (T4CP) *traG* is indicated in yellow and the putative relaxase *virD2*-like protein is indicated in brown.

T4SS, *traG*, and upstream genes involved in replication and partitioning shared synteny with the T4SS clusters on other plasmids such as *Pantoea* sp. PSNIH1 (pPSP-a3e), *Pseudomonas aeruginosa* PA96 (pOZ1760), and *Ketogulonicigenium vulgare* SKV (pKvSKV1) (Fig. 3.2B). Typically, *traG* (T4CP) is coupled to the same operon of T4SS while the region encoding replication and partitioning may be separated (Fig. 3.2B), in some cases relatively far. It is interesting to note that in two *Mesorhizobium loti* strains and *Novosphingobium* sp. PP1Y, the T4SS operon and *traG-tral* are completely separated (Fig. 3.2B). Instead, VirD2-like protein (relaxase), *traG* (T4CP) and *tral* formed a single operon.

Most of the Pseudomonadaceae-family plasmids do not contain this *trb* operon (Fig. 3.1) except for pTTS12, pOZ176 from *P. aeruginosa* PA96, pJB37 from *P. aeruginosa* FFUP_PS_37 and an unnamed plasmid from *P. aeruginosa* PA83. Therefore, this conjugative operon may not be common in IncP-2 plasmid family. However, this *trb* operon is abundant among Enterobacteriaceae-family plasmids (Fig. 3.1).

Distribution of transposable elements conferring heavy metal resistance

pTTS12 as well as many other highly similar plasmids contain a multitude of mobile genetic elements, such as ISS12 and Tn3-family transposases. pTTS12 harbors five copies of Tn3-family transposable elements; two copies of Tn3-I with highest identity to Tn4656, two copies of Tn3-II that are highly similar to Tn5053 and a single copy of Tn3-III with highest similarity to Tn5563 (Fig. 3.3A). Tn3-I is an identical transposase (RPPX_RS27515, *tnpR* and RPPX_RS27515, *tnpA*) to Tn4656 encoded on pWW53 plasmid from *P. putida* MT53. Moreover, the 39-bps inverted repeat (IR) sequences found on both ends of these two elements are highly identical with only a single mismatch difference. In addition to *tnpA* and *tnpR*, this Tn3-element contains a putative methyl-accepting chemotaxis protein (*mcpT-2*) and an insertion sequence IS256. Tn3-II of pTTS12 is identical (99.8% similarity) to Tn5053 of *Xanthomonas* sp. W17 encoding a mercury resistance gene cluster *merR* and *merTPAD* (7). This Tn3-II has 25 bp inverted repeats, bracketing the ends and 5 bp directed repeats (DR). Tn3-III is identical to Tn5563, that is found in several other plasmids, eg. pAMBL of *P. aeruginosa*, pSTY of *P. taiwanensis* VLB-120 and pRA2 of *P. alcaligenes*. The Tn3-III has identical 38 bps IRs bracketing the element, also identical to IRs found for this element in other plasmids. This element contains several genes such as *merR*, *merTP*, *piiT* and a gene with a PIN nuclease domain.

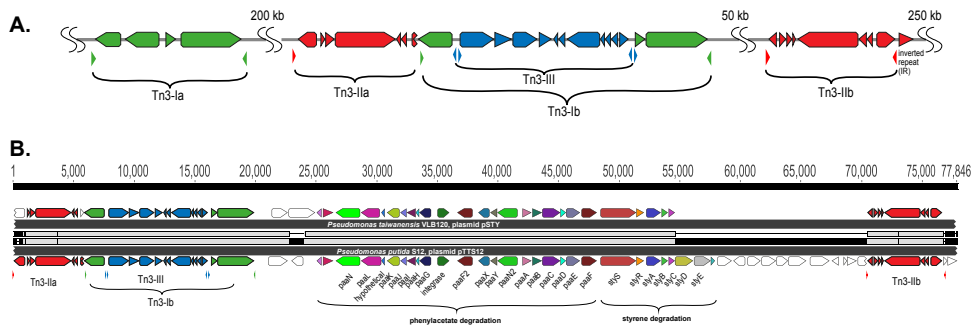


Fig. 3.3. Tn3 transposon family elements responsible for horizontal gene transfer of styrene and phenylacetate degradation pathway.

A. Genetic organization of the three different Tn3-family transposable elements in pTTs12. Colors represent the three different Tn3 transposon families; Tn3-I with highest identity to Tn4656 (green), Tn3-IIa and b with highest identity to Tn5053 (red) and Tn3-III with highest identity to Tn5563 (blue). The inverted repeats (IRs) flanking each element are marked by small lowered triangles in the same colours, accordingly.

B. Alignment of the Tn3-mediated horizontal gene transfer of the styrene and phenylacetate degradation cluster in pTTs12 (bottom) and pSTY from *Pseudomonas taiwanensis* VLB120 (top). Colors represent the different genes constituting styrene-phenylacetate degradation cluster and the three Tn3 transposable elements, corresponding to the color-coding in panel A. Gene names are indicated.

The Tn4656 and Tn5563 are both duplicated and rearranged on the megaplasmid together with Tn5053. This rearrangement resulted in a highly characteristic sequence, which partially resulted from insertion of Tn5053 transposition in the second copy of Tn4656 (Tn4656-II), between the *mcpT-2* and *tnpR* loci (Fig. 3.3). The IRs as well as DRs of Tn5053 indicate the insertion site of this element. The IRs of Tn4656-II are well preserved bracketing both elements. Other parts of this sequence consist of the second copy of Tn5563 (Tn5563-II), which is truncated at the right end by insertion of Tn4656-II in *merT* and thus truncated the 5' end of *merT* sequence, can be identified. Due to this truncation, the IRs of Tn4656-II cannot be found on the right side of the element anymore except for the right IR of initial Tn4656, which is located 58 kbps upstream of this element.

The unique rearrangement of the three different Tn3 elements in pTTs12 surprisingly is also present on pSTY of *P. taiwanensis* VLB120, including an additional copy of Tn5563. In between these two Tn5563-elements, both megaplasmids contain the complete styrene degradation pathway, enabling both strains to grow on styrene as sole carbon source (25, 30). Detailed comparison of the regions between the two Tn5563 elements from pTTs12 and

pSTY reveals a high similarity between Tn5563-I and Tn5563-II (Fig. 3.3B). This sequence is around 77 kbps and 60 kbps for pTTS12 and pSTY respectively, including the IRs bracketing both sequences.

In addition to Tn3-elements, a unique Tn7-like element (20 kbps) is also encoded on pTTS12 (Fig. 3.1). Interestingly, an identical transposable element is also encoded on the chromosome of *P. putida* S12. This element contains several transposase genes at both ends and a putative chromate resistance gene cluster (locus tag RPPX_28930-29030). The putative chromate resistance gene cluster was identified based on homology search using BLAST and alignments to other plasmids. RPPX_28995, RPPX_28990, and RPPX_29000 were identified to encode for a chromate resistance efflux pump ChrA, and two regulatory proteins ChrB and ChrF respectively similar to the chromate resistance gene cluster carried by pMOL28 of *Cupriavidus metallidurans* CH34 (33).

Conjugative megaplasmid pTTS12 is highly stable in *P. putida* KT2440

To characterize the conjugative transferability of pTTS12, we performed biparental mating between *P. putida* S12.1 and *P. putida* KT-BG35. *P. putida* KT-BG35 is a strain derived from *P. putida* KT2440, does not harbour a megaplasmid and carries a gentamicin resistant marker and green fluorescence protein (GFP) at its *attn7* site (34). The transfer was performed using biparental mating between *P. putida* S12.1 containing pTTS12 with kanamycin resistant marker and *P. putida* KT-BG35. Transconjugant colonies resistant to both kanamycin and gentamicin occurred at the frequency of $4.20 (\pm 0.51) \times 10^{-7}$. After appropriate selection on agar plates, the identity of transconjugant colonies was confirmed by observing GFP expression of the colonies derived from *P. putida* KT-BG35. Additionally, transfer of entire pTTS12 was confirmed using PCR. Amplification of several regions of pTTS12 using primer pairs 53,496_Fw-56,596_Rv, 200,497_Fw-203,602_Rv, and 286,448_Fw-289,462_Rv resulted in an expected band of 3 kbp in transconjugant colonies. All 15 randomly selected colonies chosen for colony PCR showed correct bands. This confirmed the transfer of entire pTTS12 into *P. putida* KT-BG35 and the resulting strains will further be referred to as *P. putida* KTpS12. Several attempts to transfer pTTS12 into *E. coli* strains represented by *E. coli* MV1190 and *E. coli* XL1-Blue by biparental mating did not result in any successful transconjugant colonies.

The putative relaxase gene, *virD2*, was identified on pTTS12 (locus tag RPPX_28750). To confirm this finding, we created a complete deletion of *virD2* gene and compared the self-transfer frequency of pTTS12 Δ *virD2* and wild-type pTTS12 into *P. putida* KT2440. The transfer frequency of pTTS12 Δ *virD2* was $4.16 (\pm 0.08) \times 10^{-7}$, which was not significantly different (p-value 0.8867) compared to the transferability of the wild-type pTTS12 from *P. putida* S12 to *P. putida* KT2440.

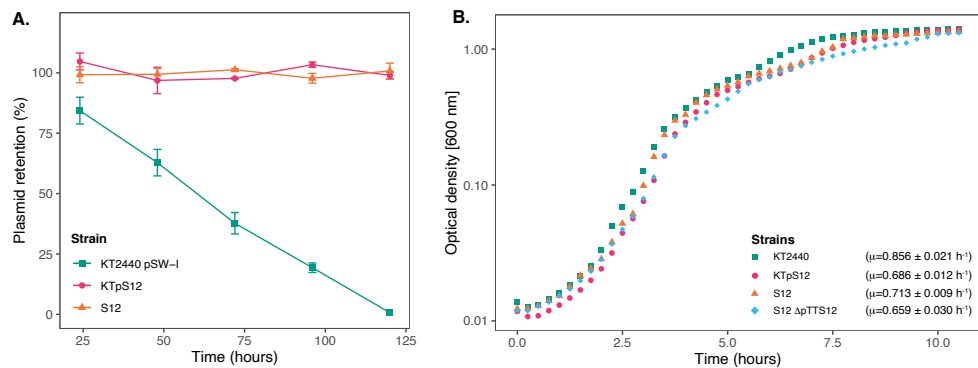


Fig. 3.4. Megaplasmid pTTS12 is highly stable in *P. putida* strains and reduces maximal growth rate in *P. putida* KT2440.

A. Plasmid retention of pTTS12 in *P. putida* KT2440 and *P. putida* S12 on liquid LB without selection pressure for approximately 50 generations. Colors and shapes indicate the different strains with green squares indicating *P. putida* KT2440 pSW-II, magenta circles indicating *P. putida* KTpS12, and orange triangles indicating *P. putida* S12 (containing pTTS12). Plasmid pSW-II in *P. putida* KT2440 was used as a control for loss of unstable plasmid. pTTS12 is stably maintained in both *P. putida* S12 and *P. putida* KTpS12.

B. Growth curve of *P. putida* KT2440, *P. putida* KTpTTS12, *P. putida* S12, and *P. putida* S12 Δ pTTS12. Growth was followed on liquid LB at 30 °C, 200 rpm shaking. Growth curves represent data obtained from three biological replicates for each strain, starting from $OD_{600\text{nm}} = 0.05$. Green squares indicate *P. putida* KT2440 pSW-II, magenta circles indicate *P. putida* KTpS12, orange triangles indicate *P. putida* S12 (containing pTTS12), and blue diamond indicate *P. putida* S12 Δ pTTS12. Maximum growth rates calculated for each strain are indicated within the figure.

The stability of pTTS12 in *P. putida* KTpS12 and *P. putida* S12 was examined for 5 passages in the absence of antibiotic selective pressure (approximately 10 generations/passage step). No plasmid loss was observed from either *P. putida* KTpS12 or *P. putida* S12 growing without selective pressure while the negative control pSW-2 showed a steady plasmid loss (Fig. 3.4A). Serendipitous deletion of pTTS12 was not found in *P. putida* S12 and *P. putida* KTpS12 either. Hence, pTTS12 is a stable megaplasmid in both *P. putida* S12 and *P. putida* KT2440.

putida KT2440.

The occurrence of large plasmids in bacteria is known to cause metabolic burden, which is reflected in reduced bacterial growth rate (μ). *P. putida* KTpS12 exhibited a lower maximum growth rate compared to *P. putida* KT2440, 0.686 ± 0.012 and $0.856 \pm 0.021 \text{ h}^{-1}$ respectively (Fig. 3.4B). However, *P. putida* S12 and *P. putida* S12 Δ pTTS12 did not show a significant maximum growth rate difference (0.713 ± 0.009 and $0.659 \pm 0.030 \text{ h}^{-1}$ respectively). The length of lag-phase and biomass yield at stationary phase remained unaffected with pTTS12 present in both *P. putida* S12 and KTpS12. Apparently, the presence pTTS12 imposes a only slight metabolic burden in *P. putida* KT2440, but not in S12.

Phenotypic features of pTTS12 and attained solvent tolerance in *P. putida* KT2440

P. putida S12 is intrinsically tolerant to an assortment of environmental xenobiotics. The majority of these characteristic traits are encoded on pTTS12; the styrene degradation operon *styABCDE*, the tellurite resistance operon *terZABCDE* and a solvent efflux pump *srpABC*. To explore functionality of pTTS12 following conjugative transfer, these characteristic traits were investigated in *P. putida* KTpS12 (Fig. 3.5). Activity of the styrene degradation operon in *P. putida* KTpS12 was tested by growing on minimal media with styrene as carbon source and inspecting transformation of indole into indigo. Similarly as observed in *P. putida* S12, *P. putida* KTpS12 was able to transform indole into indigo, whereas wild-type KT2440 was not, indicating activity of styrene monooxygenase (*styA*) and styrene oxide isomerase (*styB*) in these strains (Fig. 3.5A). In addition, *P. putida* KTpS12 was able to grow on minimal media supplemented with styrene as carbon source or minimal media agar plates incubated in styrene atmosphere (data not shown).

Potassium tellurite (K_2TeO_3) exhibits antimicrobial activity and tellurite resistance in bacteria is achieved through reduction of tellurite (TeO_3^{2-}) into a less toxic metallic tellurium (Te^0), hence the formation of black colonies in the presence of tellurite (35). The resistance genes on pTTS12 are encoded as an operon *terZABCDE* (RPPX_26360-26385). To investigate whether this gene cluster is able to increase resistance towards tellurite in *P. putida* KT2440, the minimum inhibitory concentration (MIC) was determined for the three different stains (Fig. 3.5B). The MIC of potassium tellurite for *P. putida* KT2440 was 16 fold less compared to *P. putida* S12, $12.5 \text{ mg liter}^{-1}$ and $200 \text{ mg liter}^{-1}$ respectively. Interestingly, *P. putida*

KTpS12 showed an 8 fold increase in tellurite resistance (MIC 100 mg liter⁻¹) compared to its parental strain *P. putida* KT2440.

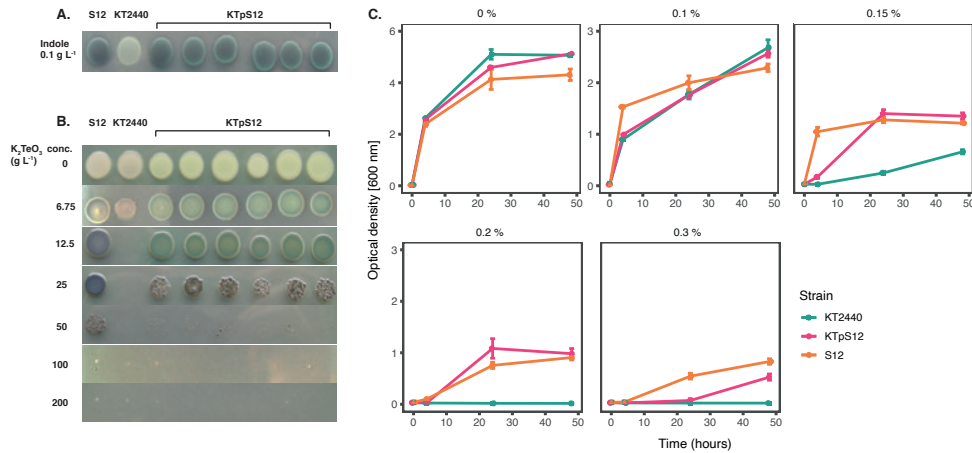


Fig. 3.5. Transfer of pTTS12 phenotypic characteristics.

A. Production of indigo from indole indicating activity of styrene monooxygenase (StyA) and styrene oxide isomerase (StyB). Minimal medium (M9) was supplemented with indole which, in the presence of StyAB enzymes encoded on pTTS12, is converted into indigo. Positive control *P. putida* S12 showed indigo coloration, whereas negative control *P. putida* KT2440 remained white. *P. putida* KTpS12 showed indigo coloration indicating activity of pTTS12-encoded *styAB*.

B. Growth of *P. putida* strains in the presence of potassium tellurite (K₂TeO₃). Minimum inhibitory concentration (MIC) of positive control *P. putida* S12 was 200 g liter⁻¹ whereas the MIC of the wild-type *P. putida* KT2440 was 12.5 g liter⁻¹. The MIC of *P. putida* KTpS12 was 100 g liter⁻¹ indicating the presence and activity of the *ter* operon on pTTS12.

C. Growth of *P. putida* strains on increasing concentrations of toluene. Optical density (OD_{600nm}) of the cultures was measured at 4, 24, and 48-hour time points with starting point of OD_{600nm} = 0.1. The y-axis range is different between the first panel (0-6) and the other panels (0-3). Green squares indicate *P. putida* KT2440 pSW-II, magenta circles indicate *P. putida* KTpS12, and orange triangles indicate *P. putida* S12 (containing pTTS12). *P. putida* KTpS12 showed an increase in solvent tolerance indicating the presence and activity of the *srp* operon from pTTS12.

The solvent efflux pump *srpABC* encoded on the megaplasmid pTTS12, enables survival and growth of *P. putida* S12 in non-utilized organic solvents (36). In order to investigate the effect of induced tolerance toward organic solvents due to the introduction of pTTS12 in *P. putida* KTpS12, a growth assay was performed in the presence of different toluene concentrations (Fig. 3.5C). *P. putida* KT2440 was able to grow in LB liquid media supplemented

with toluene up to a maximum of 0.15 % (vol/vol) concentration, although suffering from a significant growth reduction compared to *P. putida* S12. With the introduction of pTTS12, *P. putida* KTpS12 tolerance toward toluene increased to 0.30 % (vol/vol). Similar concentration was obtained for *P. putida* S12, while *P. putida* KTpS12 exhibited slightly slower growth in the presence of toluene. These observations indicated that the introduction of megaplasmid pTTS12 provided a full set of characteristic features to *P. putida* KT2440.

Discussion

Megaplasmid pTTS12 defines an environment-adaptive and type-specific family of IncP-2 plasmids, carrying distinct accessory gene clusters

Megaplasmid pTTS12 of *P. putida* S12 is closely related to other plasmids in proteobacteria, especially within the *Pseudomonas* genus. In this study we demonstrated high similarity of the pTTS12 'backbone' with pOZ176 from *P. aeruginosa* PA96 (2) and several other IncP-2 plasmids, such as pQBR103 of *Pseudomonas fluorescens* SBW25 (37). pOZ176 has been categorized within incompatibility group IncP-2 based on its replication, partitioning, and transfer machinery along with conferring tellurite resistance as a key feature of IncP-2 plasmid (2, 5). Indeed, pTTS12 encodes typical characteristics of IncP-2 plasmids, such as heavy metal resistance (tellurite, mercury, and chromate) and plasmid maintenance via the *parA/parB/repA* system (10, 38). pTTS12 clearly conferred tellurite resistance when transferred to tellurite-susceptible *P. putida* KT2440, confirming this IncP-2 characteristic phenotype. Interestingly, despite high similarity between pTTS12 and pOZ176, pTTS12 lacks the Tn6016 *bla*_{IMP-9}-carrying class 1 integron cassette which is an important trait of pOZ176 conferring resistance to aminoglycosides and carbapenems (2, 5). On the other hand, pOZ176 lacks the solvent efflux pump, styrene degradation pathway, and phenylpropionic acid degradation pathway which are main characteristics of pTTS12. This demonstrates that very similar megaplasmid backbones may carry resistance to a diversity of xenobiotics, metabolic functions, or virulence gene clusters (39). Whereas the traits disseminated by pTTS12 and pOZ176 respectively, are highly divergent and distinctive, a similar observation of environment-adaptive traits conferred by flexible and diverse accessory gene clusters contained on IncP-2 plasmids was recently reported for *P. aeruginosa* plasmids pBT2436 and pBT2101, carrying multiple MDR cassettes (1).

Convergent distribution of plasmid-encoded solvent tolerance gene clusters

pTTS12 shares its unique features of styrene and phenyl-propanoate degradation pathway with *P. taiwanensis* VLB120 and the solvent extrusion pump SrpABC with TtgGHI from *P. taiwanensis* VLB120 and *P. putida* DOT-T1E. These solvent tolerant strains were isolated independent of each other, although in different geographical locations; *P. putida* S12 and *P. taiwanensis* VLB120 were isolated for their ability to utilize styrene as sole carbon source (11, 40). *P. putida* DOT-T1E was isolated for its ability to degrade toluene (9). Hence, these plasmids isolated from different environmental sources show convergent distribution of highly similar gene clusters with similar features related to environmental stresses (e.g. organic solvents) on different plasmid backbones. In *P. taiwanensis* VLB120, the arrangement of gene clusters encoding the styrene degradation pathway and solvent efflux pump - phenylpropionic acid degradation pathway is highly similar to pTTS12, with 99% and 80% similarity, respectively. This moreover, indicates that exchange of the styrene degradation pathway occurred more recently than exchange of the efflux pump/phenylpropionic acid degradation cluster. Alternatively, these clusters may have been acquired independently.

The styrene degradation gene cluster is encoded within a unique arrangement of Tn3 family transposases shared by pTTS12 and pSTY from *P. taiwanensis* VLB120 (Fig. 3.3). Due to the transposition of Tn3-Ib, Tn3-IIa lost its right flank inverted repeat (IR). Because of this arrangement, Tn3-IIa can only “jump” while carrying the entire Tn3 and styrene-phenylacetate degradation clusters using the right flank of Tn3-IIb IR. This may explain the occurrence of the styrene-phenylacetate degradation cluster distinctive arrangement shared between pTTS12 and pSTY. Although we could not find evidence of mobile genetic elements carrying the efflux pump and the phenylpropionic acid degradation gene clusters on pSTY and pTTS12, it is well possible that the exchange originally occurred via such route.

Transferability of pTTS12

pTTS12 contains a P-Type type IV secretion system (T4SS) with synteny similar to the prototype *trb* operon of the *A. tumefaciens* pTiC58 system (32, 41). Indeed, our experiments showed that pTTS12 is transferable towards other *P. putida* strains with a frequency of 4.20 (\pm 0.51) \times 10⁻⁷. A putative relaxase, responsible for creating a nick prior to plasmid transfer via the conjugative bridge, was predicted to be encoded by *virD2* (locus tag RPPX_28750). However, complete deletion of *virD2* did not resulted in a significant reduction of transfer frequency,

compared to the wild-type pTTS12. This may indicate the presence of other relaxase(s) which act in-trans with the P-type T4SS to mediate the nicking of plasmid DNA and subsequently aided the plasmid transfer process. *P. putida* S12 contains other T4SS within its genome which share synteny with the I-type T4SS represented by Dot/lcm from *L. pneumophila* (Fig. 3.S3), although it is unclear whether Dot/lcm can support the transfer of pTTS12 (42).

Amelioration of pTTS12 reduces fitness cost and promotes plasmid persistence in *P. putida* S12

We observed that in its original host *P. putida* S12 on rich media, pTTS12 did not impose an apparent metabolic burden whereas in another strain as *P. putida* KT2440, pTTS12 caused a 20% reduction of maximum growth rate. We previously reported on the occurrence of metabolic burden caused by pTTS12 in *P. putida* S12 in the presence of toluene (43). In addition to the relatively low metabolic burden, pTTS12 was very stable in both *P. putida* S12 and *P. putida* KT2440 (Fig. 3.4A). Several mechanisms may be involved in the reduced fitness cost and the stability of pTTS12 in *P. putida* S12.

Conjugative transfer may impose substantial cost and burden due to the energy investment on pili formation during conjugation (39, 44). Indeed, pTTS12 showed a substantially lower conjugation rate (4.20×10^{-7} transfer frequency) after 24 hours in comparison to other IncP-2 plasmids (10^{-1} to 10^{-4} transfer frequency after 2 hours) (38). Downregulation of plasmid genes appeared to be involved in the amelioration of pTTS12. The expression of plasmid-encoded resistance genes, like the solvent extrusion pump, can typically be a source of metabolic burden imposed by plasmids (45). pTTS12 contains multiple types of mobile genetic elements, with ISS12 being the most abundant (4, 27). Substantial duplication of the ISS12 mobile element has previously been reported to interrupt *srpA*, encoding the periplasmic subunit of the solvent efflux pump (4). In the prolonged absence of organic solvent, expression and maintenance of the solvent efflux pump may be costly for the bacterial cell, hence, interruption of the *srp* efflux pump gene cluster may further reduce the plasmid burden of pTTS12. In addition to these mechanisms, we recently described the contribution of a toxin-in-antitoxin module SlvT-SlvA to the stability of pTTS12 (43).

Future outlook

IncP-2 family plasmids are widely distributed among environmental and clinical *Pseudomonas* isolates. These plasmids contain variable regions encoding MDR, xenobiotics extrusion

pumps, degradation pathways, and heavy metal resistance cassettes. In contrast to the dynamic variable regions, the core backbone of these plasmids shows a general conservation. It is interesting to discover the minimal backbone of IncP-2, which enables Pseudomonads to scavenge gene clusters important for its survival both in environmental and clinical set-up, as a model of horizontal gene transfer. Ultimately, IncP-2 plasmid backbone may be promising for biotechnological and bioremediation applications due to its stability and relatively low metabolic burden. Moreover, these plasmids have been described to exchange their traits, thus creating hybrid plasmids when they occur within the same host (38). The mechanisms for such exchange are poorly understood and may well involve transposition and conjugation as suggested by the shared and type-specific characteristics of pTTS12 and pOZ176 as described in this study. Further clarification of these mechanisms is important to shed light on the rapid dissemination of bacterial tolerance and resistance to antibiotics and chemical stresses in the environment.

Successful attempts have been made in exploiting traits from environmental plasmids for standardized components in synthetic biology (46). Environmental plasmids are exchangeable between different hosts and may express their genetic features in various genomic and metabolic backgrounds. Moreover, they are an excellent source of novel biological parts such as origin of replication, metabolic pathway, resistance marker, and regulated promoters. New sequencing technologies and comparative genomics analyses support the identification of the genes enabling these features. Here, we demonstrated that pTTS12 contains promising exchangeable gene clusters and building blocks to construct robust microbial hosts for high-value biotechnology applications.

Materials and methods

Cultivation of *P. putida*

Table 3.2. Bacterial strains and plasmids used in this study

Strain/plasmid	Relevant characteristics	Ref.
<i>E. coli</i> DH5α	<i>sup</i> E44, $\Delta lacU169$ ($\Phi lacZ\Delta M15$), <i>recA1</i> , <i>endA1</i> , <i>hsdR17</i> , <i>thi-1</i> , <i>gyrA96</i> , <i>relA1</i>	(52)
<i>E. coli</i> DH5α λpir	<i>sup</i> E44, $\Delta lacU169$ ($\Phi lacZ\Delta M15$), <i>recA1</i> , <i>endA1</i> , <i>hsdR17</i> , <i>thi-1</i> , <i>gyrA96</i> , <i>relA1</i> , λpir phage lysogen	(53)
<i>E. coli</i> HB101	<i>recA pro leu hsdR Sm^R</i>	(54)

Strain/plasmid	Relevant characteristics	Ref.
<i>E. coli</i> XL-1 Blue	endA1 gyrA96(nalR) thi-1 recA1 relA1 lac glnV44 F' [::Tn10 proAB+ lacIq Δ(lacZ)M15] hsdR17(rK- mK+) Tc ^R	Stratagene
<i>E. coli</i> MV1190	delta(lacproAB) thi supE44 delta(sr1recA)306::Tn10 [F':traD36 proAB lacIq delta(lacZ)M15] Tc ^R	ATCC
<i>P. putida</i> KT2440	Derived from wild-type <i>P. putida</i> mt-2, Δ _{pWW0}	(55)
<i>P. putida</i> S12	Wild-type <i>P. putida</i> S12 (ATCC 700801), harboring megaplasmid pTTS12	(11)
<i>P. putida</i> S12.1	<i>P. putida</i> S12; Km ^R on pTTS12	This paper
<i>P. putida</i> KT-BG35	<i>P. putida</i> KT2440; Gm ^R , msfgfp::Tn7	This paper
<i>P. putida</i> KTpS12	<i>P. putida</i> KT2440, Gm ^R , msfgfp::Tn7, pTTS12, Km ^R	This paper
pRK2013	RK2-Tra ⁺ , RK2-Mob ⁺ , Km ^R , ori ColE1	(56)
pTTS12	A 583 kbp megaplasmid of <i>P. putida</i> S12	(25)
pTnS-1	Ap ^R , ori R6K, TnSABCD operon	(57)
pBG35	Km ^R , Gm ^R , ori R6K, pBG-derived	(34)
pEMG	Km ^R , Ap ^R , ori R6K, lacZα MCS flanked by two I-SceI sites	(48)

Strains and plasmids used in this report were listed in Table 3.2. All *P. putida* strains were grown in Lysogeny Broth (LB) containing 10 g liter⁻¹ tryptone, 5 g liter⁻¹ yeast extract and 5 g liter⁻¹ sodium chloride at 30 °C with 200 rpm shaking. *E. coli* strains were cultivated in LB at 37 °C with 250 rpm shaking in a horizontal shaker (Innova 4330, New Brunswick Scientific). For solid cultivation, 1.5 % (wt/vol) agar was added to LB. M9 minimal medium used in this report was supplemented with 2 mg liter⁻¹ MgSO₄ and 0.2% (wt/vol) of citrate as sole carbon source (11). Bacterial growth was observed by optical density measurement at 600 nm (OD_{600nm}) using a spectrophotometer (Ultraspec 2100 pro, Amersham Biosciences). Maximum growth rate and other parameters were calculated using growthcurver R-package ver.0.3.0 (47). Solvent tolerance analysis was performed by growing *P. putida* strains in LB starting from OD_{600nm} = 0.1 in Boston bottles with Mininert bottle caps. When required, potassium tellurite (6.75 - 200 mg liter⁻¹), indole (100 mg liter⁻¹), gentamicin (25 mg liter⁻¹), ampicillin (100 mg liter⁻¹), tetracycline (25 mg liter⁻¹), and kanamycin (50 mg liter⁻¹) were added to the media.

DNA methods

All PCR reaction were performed using Phire polymerase (Thermo Fischer) according to the manufacturer's manual. All primers are listed in Table 3.3 and were obtained from Sigma-Aldrich. PCR reactions were visualized and analyzed by gel electrophoresis on 1 % (wt/vol) TBE agarose gels containing 5 mg liter⁻¹ ethidium bromide in an electric field (110V, 0.5x TBE running buffer).

Table 3.3. Primers used in this study

Primer	Sequence	Target
glmS_Fw	AGTCAGAGTTACGGAATTGTAGG	<i>P. putida</i> KT2440 (Tn7 site)
glmS_Rv	GTCGAGAAAAATTGCCGAGCT	<i>P. putida</i> KT2440 (Tn7 site)
53,496_Fw	ACTTCGACCAATGCCATT	<i>P. putida</i> S12 pTTS12
56,596_Rv	GGACACCCCTCATCCTTAGCG	<i>P. putida</i> S12 pTTS12
200,497_Fw	GTGTATCGAAGGGCCTCCAC	<i>P. putida</i> S12 pTTS12
203,602_Rv	TCGACGATGCAGACAGATCG	<i>P. putida</i> S12 pTTS12
286,448_Fw	AACACCGAAGATGGGGCTT	<i>P. putida</i> S12 pTTS12
289,462_Rv	GCAGGTCGACAAGCAAGTTG	<i>P. putida</i> S12 pTTS12
4,963,661_Fw	ATCACCCAGCTGAGCCATT	<i>P. putida</i> S12 chromosome
4,966,726_Rv	CTGCCGGATAACAAAGCAGC	<i>P. putida</i> S12 chromosome
90285_Fw	TTT <u>TCTAGA</u> TGCTGAGCAGTT CCTTCAGG	Construction of pEMG-TS for Km ^R marker in pTTS12, with XbaI restriction site
90825_Rv	TTT <u>CCCGGG</u> GAGGAAGGGAAAG CAAACCTCCG	Construction of pEMG-TS for Km ^R marker in pTTS12, with XmaI restriction site
TS1_28750_Fw	AATCT <u>GAATT</u> CGGACGTATTG GGCTTCAATG	Construction of pEMG-Δ28750 for deleting the putative relaxase, with EcoRI restriction site
TS1_28750_Rv	GAAAGCCTGTCTGCACATGG CTATCGACTCATCATTACCG	Construction of pEMG-Δ28750 for deleting the putative relaxase
TS2_28750_Fw	CGGTGAATGATGAGTCGATCA TGTGCAGACAGGCTTC	Construction of pEMG-Δ28750 for deleting the putative relaxase
TS2_28750_Rv	AACCC <u>GGATCC</u> GTTCGACA GCCGCTATTTC	Construction of pEMG-Δ28750 for deleting the putative relaxase, with BamHI restriction site
test_28750_Fw	CCTGATGCACGATTACCG	Confirming the deletion of the putative relaxase (ΔRPPX_28750)
test_28750_Fw	CTACCTGCCGGTACACATT	Confirming the deletion of the putative relaxase (ΔRPPX_28750)

Megaplasmid pTTS12 transfer into *P. putida* KT2440 and *E. coli* strains

Gentamicin resistance and GFP containing cassette were incorporated into *P. putida* KT2440 chromosome at the Tn7 site using pBG35 plasmid resulting in the strain *P. putida* KT-BG35 as previously described (34). Correct transformants were additionally verified by observing the gentamicin resistance, GFP expression and colony PCR of *P. putida* KT2440 chromosome sequence. Kanamycin resistance gene was introduced into the megaplasmid pTTS12 by integrating plasmid pEMG using homologous recombination resulting in *P. putida* S12.1 as previously described (48). A single homologous recombination site was obtained by PCR with 90285_Fw and 90825_Rv primer pair and this fragment was used to construct pEMG-TS plasmid. Correct integration into *P. putida* S12 was verified by observing kanamycin resistance

and colony PCR using primers 4,963,661_Fw-4,966,726_Rv.

The transfer of pTTS12 into *P. putida* KT-BG35, *E. coli* XL1-Blue or *E. coli* MV1190 were performed by biparental mating between *P. putida* S12.1 and the recipient strain on LB agar for 24 hours at 30 °C. The correct transformants were selected using LB agar supplemented with gentamicin and kanamycin for *P. putida* KT-BG35 or with tetracycline and kanamycin for *E. coli* strains. Additionally, transformants were verified using colony PCR (53,496_Fw-56,596_Rv, 200,497_Fw-203,602_Rv, and 286,448_Fw-289,462_Rv). Plasmid transfer rate was determined by comparing the event of successful plasmid transconjugant with the colony formation unit (cfu) of the recipient strain (*P. putida* KT-BG35, *E. coli* XL1-Blue or *E. coli* MV1190) after biparental mating (Gm^R/Tc^R). Plasmid stability was determined by calculating the event of megaplasmid loss in *P. putida* KTpS12 grown in liquid media without supplementation of kanamycin as the selective pressure for pTTS12. Plasmid pSW-2 was used as a control for megaplasmid loss events (48).

Sequence analyses

All plasmid sequences were downloaded from NCBI database, 22389 plasmid sequences from Refseq database (retrieved 8 March 2020) and complemented with few plasmid sequences from NUCORE that were omitted from Refseq. The CGviewer (31) was used to generate circular plots of entire pTTS12 with standard settings and MultiGeneBlast tool (49) was used to generate synteny plots of specific regions and operons. Further analysis was performed using Geneious software (BioMatters), and selected sequences were aligned using MAFFT (50) for DNA sequences or MUSCLE (51) for protein sequences.

References

1. Cazares A, Moore MP, Hall JPJ, Wright LL, Grimes M, Emond-Rhéault JG, Pongchaiskul P, Santanirand P, Levesque RC, Fothergill JL, Winstanley C. 2020. A megaplasmid family driving dissemination of multidrug resistance in *Pseudomonas*. *Nat Commun* 11:1370.
2. Xiong J, Alexander DC, Ma JH, Deraspe M, Low DE, Jamieson FB, Roy PH. 2013. Complete Sequence of pOZ176, a 500-Kilobase IncP-2 Plasmid Encoding IMP-9-Mediated Carbapenem Resistance, from Outbreak Isolate *Pseudomonas aeruginosa* 96. *Antimicrob Agents Chemother* 57:3775–3782.
3. Molina L, Duque E, Gómez MJ, Krell T, Lacal J, García Puente A, García V, Matilla MA, Ramos J-L, Segura A. 2011. The pGRT1 plasmid of *Pseudomonas putida* DOT-T1E encodes functions relevant for survival under harsh conditions in the environment. *Environ Microbiol* 13:2315–2327.
4. Hosseini R, Kuepper J, Koebbing S, Blank LM, Wierckx N, de Winde JH. 2017. Regulation of solvent tolerance in *Pseudomonas putida* S12 mediated by mobile elements. *Microb Biotechnol* 10:1558–1568.
5. Xiong J, Hynes MF, Ye H, Chen H, Yang Y, M'Zali F, Hawkey PM. 2006. *bla*_{IMP-9} and its association with large plasmids carried by *Pseudomonas aeruginosa* isolates from the People's Republic of China. *Antimicrob Agents Chemother*.
6. Nojiri H, Shintani M, Omori T. 2004. Divergence of mobile genetic elements involved in the distribution of xenobiotic-catabolic capacity. *Appl Microbiol Biotechnol* 64:154–174.
7. Kholodii GY, Yurieva O V, Lomovskaya OL, Gorlenko ZM, Mindlin SZ, Nikiforov VG. 1993. Tn5053, a mercury resistance transposon with integron's ends. *J Mol Biol* 230:1103–1107.
8. Partridge SR, Kwong SM, Firth N, Jensen SO. 2018. Mobile genetic elements associated with antimicrobial resistance. *Clin Microbiol Rev* 31:e00088-17.
9. Ramos JL, Duque E, Huertas MJ, Haïdour A. 1995. Isolation and expansion of the catabolic potential of a *Pseudomonas putida* strain able to grow in the presence of high concentrations of aromatic hydrocarbons. *J Bacteriol* 177:3911–3916.
10. Shintani M, Sanchez ZK, Kimbara K. 2015. Genomics of microbial plasmids: classification and identification based on replication and transfer systems and host taxonom-

my. *Front Microbiol* 6:242.

11. Hartmans S, van der Werf MJ, de Bont JA. 1990. Bacterial degradation of styrene involving a novel flavin adenine dinucleotide-dependent styrene monooxygenase. *Appl Environ Microbiol* 56:1347–1351.
12. Kieboom J, Dennis JJ, de Bont JAM, Zylstra GJ. 1998. Identification and Molecular Characterization of an Efflux Pump Involved in *Pseudomonas putida* S12 Solvent Tolerance. *J Biol Chem* 273:85–91.
13. Kusumawardhani H, Hosseini R, de Winde JH. 2018. Solvent Tolerance in Bacteria: Fulfilling the Promise of the Biotech Era? *Trends Biotechnol* 36:1025–1039.
14. Mukhopadhyay A. 2015. Tolerance engineering in bacteria for the production of advanced biofuels and chemicals. *Trends Microbiol* 23:498–508.
15. Janardhan Garikipati SVB, Peeples TL. 2015. Solvent resistance pumps of *Pseudomonas putida* S12: Applications in 1-naphthol production and biocatalyst engineering. *J Biotechnol* 210:91–99.
16. Koopman F, Wierckx N, de Winde JH, Ruijssenaars HJ. 2010. Efficient whole-cell biotransformation of 5-(hydroxymethyl)furfural into FDCA, 2,5-furandicarboxylic acid. *Bioresour Technol* 101:6291–6296.
17. Verhoef S, Wierckx N, Westerhof RGM, de Winde JH, Ruijssenaars HJ. 2009. Bioproduction of p-hydroxystyrene from glucose by the solvent-tolerant bacterium *Pseudomonas putida* S12 in a two-phase water-decanol fermentation. *Appl Environ Microbiol* 75:931–936.
18. Verhoef S, Ruijssenaars HJ, de Bont JAM, Wery J. 2007. Bioproduction of p-hydroxybenzoate from renewable feedstock by solvent-tolerant *Pseudomonas putida* S12. *J Biotechnol* 132:49–56.
19. Wierckx NJP, Ballerstedt H, de Bont JAM, Wery J. 2005. Engineering of solvent-tolerant *Pseudomonas putida* S12 for bioproduction of phenol from glucose. *Appl Environ Microbiol* 71:8221–8227.
20. Kieboom J, Dennis JJ, Zylstra GJ, de Bont JA. 1998. Active efflux of organic solvents by *Pseudomonas putida* S12 is induced by solvents. *J Bacteriol* 180:6769–6772.
21. Volkers RJM, Snoek LB, Ruijssenaars HJ, de Winde JH. 2015. Dynamic Response of *Pseudomonas putida* S12 to Sudden Addition of Toluene and the Potential Role of the Solvent Tolerance Gene *trgl*. *PLoS One* 10:e0132416.

22. Rühl J, Hein E-M, Hayen H, Schmid A, Blank LM. 2012. The glycerophospholipid inventory of *Pseudomonas putida* is conserved between strains and enables growth condition-related alterations. *Microb Biotechnol* 5:45–58.

23. Wijte D, van Baar BLM, Heck AJR, Altelaar AFM. 2011. Probing the proteome response to toluene exposure in the solvent tolerant *Pseudomonas putida* S12. *J Proteome Res* 10:394–403.

24. Volkers RJM, de Jong AL, Hulst AG, van Baar BLM, de Bont JAM, Wery J. 2006. Chemostat-based proteomic analysis of toluene-affected *Pseudomonas putida* S12. *Environ Microbiol* 8:1674–1679.

25. Kuepper J, Ruijssemaars HJ, Blank LM, de Winde JH, Wierckx N. 2015. Complete genome sequence of solvent-tolerant *Pseudomonas putida* S12 including megaplasmid pTTS12. *J Biotechnol* 200:17–18.

26. Volkers RJM, Ballerstedt H, de Winde JH, Ruijssemaars HJ. 2010. Isolation and genetic characterization of an improved benzene-tolerant mutant of *Pseudomonas putida* S12. *Environ Microbiol Rep* 2:456–460.

27. Wery J, Hidayat B, Kieboom J, de Bont JA. 2001. An insertion sequence prepares *Pseudomonas putida* S12 for severe solvent stress. *J Biol Chem* 276:5700–5706.

28. Sun X, Dennis JJ. 2009. A Novel Insertion Sequence Derepresses Efflux Pump Expression and Preadapts *Pseudomonas putida* S12 for Extreme Solvent Stress. *J Bacteriol* 191:6773–6777.

29. Rodríguez-Herva JJ, García V, Hurtado A, Segura A, Ramos JL. 2007. The ttgGHI solvent efflux pump operon of *Pseudomonas putida* DOT-T1E is located on a large self-transmissible plasmid. *Environ Microbiol* 9:1550–1561.

30. Köhler KAK, Rückert C, Schatschneider S, Vorhölter FJ, Szczepanowski R, Blank LM, Niehaus K, Goessmann A, Pühler A, Kalinowski J, Schmid A. 2013. Complete genome sequence of *Pseudomonas* sp. strain VLB120 a solvent tolerant, styrene degrading bacterium, isolated from forest soil. *J Biotechnol* 168:729–730.

31. Stothard P, Wishart DS. 2005. Circular genome visualization and exploration using CGView. *Bioinformatics* 21:537–539.

32. Christie PJ, Whitaker N, González-Rivera C. 2014. Mechanism and structure of the bacterial type IV secretion systems. *Biochim Biophys Acta - Mol Cell Res* 1843:1578–1591.

3

33. Monchy S, Benotmane MA, Janssen P, Vallaey T, Taghavi S, Van Der Lelie D, Mergeay M. 2007. Plasmids pMOL28 and pMOL30 of *Cupriavidus metallidurans* are specialized in the maximal viable response to heavy metals. *J Bacteriol* 189:7417–7425.
34. Zobel S, Benedetti I, Eisenbach L, de Lorenzo V, Wierckx N, Blank LM. 2015. Tn7-Based Device for Calibrated Heterologous Gene Expression in *Pseudomonas putida*. *ACS Synth Biol* 4:1341–1351.
35. Taylor DE. 1999. Bacterial tellurite resistance. *Trends Microbiol* 7:111–115.
36. Kieboom J, de Bont JAM. 2001. Identification and molecular characterization of an efflux system involved in *Pseudomonas putida* S12 multidrug resistance. *Microbiology* 147:43–51.
37. Hall JPJ, Harrison E, Lilley AK, Paterson S, Spiers AJ, Brockhurst MA. 2015. Environmentally co-occurring mercury resistance plasmids are genetically and phenotypically diverse and confer variable context-dependent fitness effects. *Environ Microbiol* 17:5008–5022.
38. Jacoby GA, Sutton L, Knobel L, Mammen P. 1983. Properties of IncP-2 plasmids of *Pseudomonas spp.* *Antimicrob Agents Chemother* 24:168–175.
39. Harrison E, Brockhurst MA. 2012. Plasmid-mediated horizontal gene transfer is a coevolutionary process. *Trends Microbiol* 20:262–267.
40. Panke S, Witholt B, Schmid A, Wubbolts MG. 1998. Towards a biocatalyst for (S)-styrene oxide production: characterization of the styrene degradation pathway of *Pseudomonas sp.* strain VLB120. *Appl Environ Microbiol* 64:2032–2043.
41. Li PL, Hwang I, Miyagi H, True H, Farrand SK. 1999. Essential components of the Ti plasmid trb system, a type IV macromolecular transporter. *J Bacteriol* 181:5033–5041.
42. Nagai H, Kubori T. 2011. Type IVB secretion systems of *Legionella* and other gram-negative bacteria. *Front Microbiol* 2:136.
43. Kusumawardhani H, van Dijk D, Hosseini R, de Winde JH. 2020. A novel toxin-antitoxin module SlvT–SlvA regulates megaplasmid stability and incites solvent tolerance in *Pseudomonas putida* S12. *Appl Environ Microbiol* 86:e00686-20.
44. Turner PE, Cooper VS, Lenski RE. 1998. Tradeoff Between Horizontal and Vertical Modes of Transmission in Bacterial Plasmids. *Evolution (N Y)* 52:315–329.
45. R. Craig MacLean, Milan AS. 2015. Microbial Evolution: Towards Resolving the Plas-

mid Paradox. *Curr Biol* 25:R764–R767.

46. Martínez-García E, Benedetti I, Hueso A, de Lorenzo V. 2015. Mining Environmental Plasmids for Synthetic Biology Parts and Devices. *Microbiol Spectr* 3:PLAS-0033-2014.

47. Sprouffske K, Wagner A. 2016. Growthcurver: An R package for obtaining interpretable metrics from microbial growth curves. *BMC Bioinformatics* 17:172.

48. Martínez-García E, de Lorenzo V. 2011. Engineering multiple genomic deletions in Gram-negative bacteria: analysis of the multi-resistant antibiotic profile of *Pseudomonas putida* KT2440. *Environ Microbiol* 13:2702–2716.

49. Medema MH, Takano E, Breitling R. 2013. Detecting sequence homology at the gene cluster level with multigeneblast. *Mol Biol Evol* 30:1218–1223.

50. Katoh K, Standley DM. 2013. MAFFT multiple sequence alignment software version 7: Improvements in performance and usability. *Mol Biol Evol* 30:772–780.

51. Edgar RC. 2004. MUSCLE: A multiple sequence alignment method with reduced time and space complexity. *BMC Bioinformatics* 5:113.

52. Bethesda Research Laboratories. 1986. *E. coli* DH5 alpha competent cells. Focus - Bethesda Res Lab 8:9.

53. Herrero M, De Lorenzo V, Timmis KN. 1990. Transposon vectors containing non-antibiotic resistance selection markers for cloning and stable chromosomal insertion of foreign genes in gram-negative bacteria. *J Bacteriol* 172:6557–6567.

54. Boyer HW, Roulland-dussoix D. 1969. A complementation analysis of the restriction and modification of DNA in *Escherichia coli*. *J Mol Biol* 41:459–472.

55. Bagdasarian M, Lurz R, Rückert B, Franklin FCH, Bagdasarian MM, Frey J, Timmis KN. 1981. Specific-purpose plasmid cloning vectors II. Broad host range, high copy number, RSF 1010-derived vectors, and a host-vector system for gene cloning in *Pseudomonas*. *Gene* 16:237–247.

56. Figurski DH, Helinski DR. 1979. Replication of an origin-containing derivative of plasmid RK2 dependent on a plasmid function provided in trans. *Proc Natl Acad Sci* 76:1648–1652.

57. Choi K-H, Gaynor JB, White KG, Lopez C, Bosio CM, Karkhoff-Schweizer RR, Schweizer HP. 2005. A *Tn7*-based broad-range bacterial cloning and expression system. *Nat Methods* 2:443–448.

Supplementary Materials

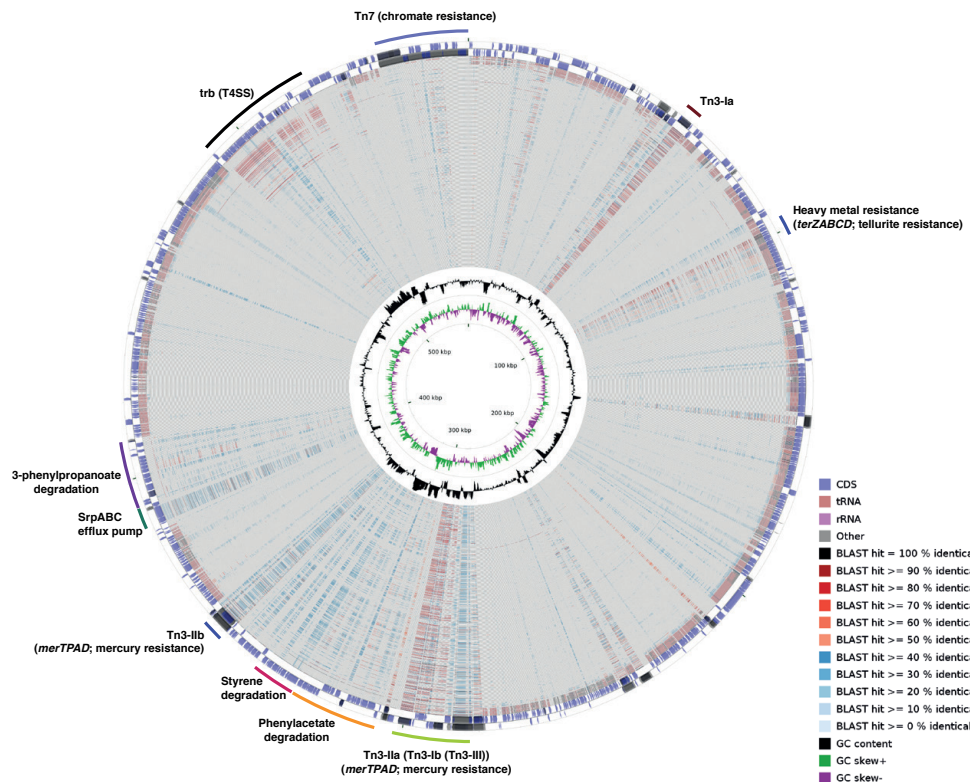


Fig. 3.S1-A. CDS alignment of the top 500 plasmids with highest similarity score to pTTS12.

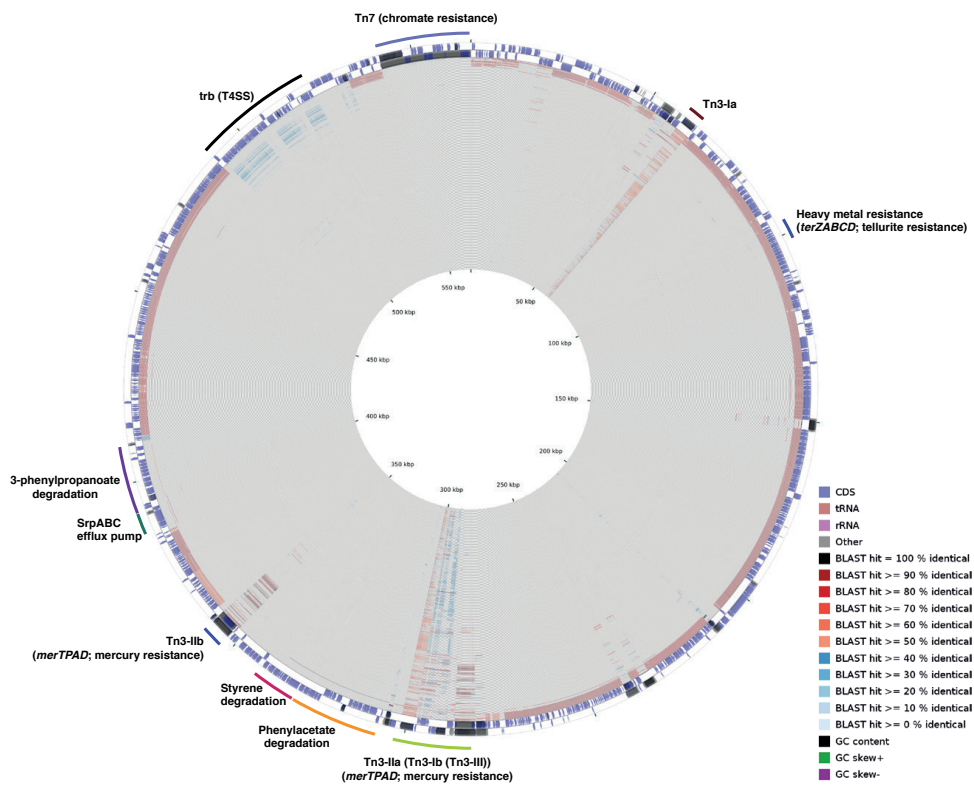


Fig. 3.S1-B. DNA alignment of the top 500 plasmids with highest similarity score to pTTS12.

Comparative analysis and elucidation of pTTS12 function

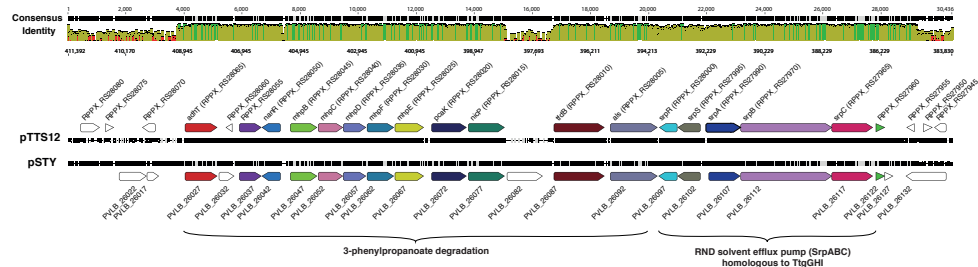
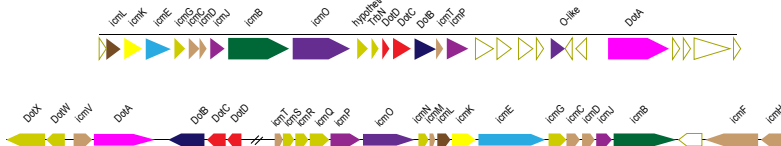


Fig. 3.S2. Comparison of the regions encoding 3-phenylpropionate degradation and solvent efflux pump between pTTS12 from *Pseudomonas putida* S12 and pSTY from *Pseudomonas taiwanensis* VLB120 reveals identical synteny and high similarity.

3



Protein	<i>C. burnetii</i> Ident./Sim.a	<i>P. putida</i> S12 Identity/Similarity	<i>P. putida</i> S12 locustag	<i>L. pneumophila</i> Locustag	Length aminoacid	Length aminoacid 2	pTTS12 Identity (%)	pTTS12 similarity (%)
IcmT	47.1/63.2	15/33	RPPX_RS13055	lpl0483	73	87	15	33
IcmS	52.6/67.5	/	—	lpl0484	—	—	—	—
IcmR	—	/	—	lpl0485	—	—	—	—
IcmQb	22.6/34.0	/	—	lpl0486	—	—	—	—
IcmP/DotM	36.5/50.3	18/38	RPPX_RS13060	lpl0487	377	437	18	38
IcmQ/DotL	59.6/70.9	28/42	RPPX_RS13025	lpl0488	784	984	28	42
IcmN/DotK	24.8/32.7	/	—	lpl0489	—	—	—	—
IcmM/DotC	—	/	—	lpl0490	—	—	—	—
IcmL/DotC	35.8/48.5	18/41	RPPX_RS12985	lpl0491	213	255	18	41
IcmK/DotH	48.2/58.6	26/40	RPPX_RS12990	lpl0492	361	338	26	40
IcmF/DotG	44.2/51.4	13/21	RPPX_RS12995	lpl0493	476	1049	13	21
IcmG/DotF	27.1/42.4	16/29	RPPX_RS13000	lpl0494	270	208	16	29
IcmC/DotE	27.7/47.1	22/38	RPPX_RS13005	lpl0495	195	195	22	38
IcmB/DotP	20.8/34.0	17/30	RPPX_RS13010	lpl0496	133	127	17	30
IcmJ/DotN	51.2/61.9	22/42	RPPX_RS13015	lpl0497	209	249	22	42
IcmB/DotO	62.2/73.7	34/54	RPPX_RS13020	lpl0498	1010	1021	34	54
IcmFf	23.1/34.4	/	—	lpl0500	—	—	—	—
IcmH	27.7/37.6	/	—	lpl0501	—	—	—	—
DotD	39.2/48.5	13/33	RPPX_RS13050	lpl2601	164	162	13	33
DotC	40.1/51.1	27/47	RPPX_RS13045	lpl2602	304	295	27	47
DotB	63.4/74.8	34/53	RPPX_RS13040	lpl2603	378	400	34	53
DotA	25.0/34.4	17/30	RPPX_RS13100	lpl2613	1048	995	17	30
IcmV	27.1/44.5	/	—	lpl2614	—	—	—	—
IcmW	58.6/68.4	/	—	lpl2615	—	—	—	—
IcmX	21.9/30.2	/	—	lpl2616	—	—	—	—

Fig. 3.S3. Type 4 secretion system encoded on *P. putida* S12 chromosome belongs to I-type, similar to prototype *L. pneumophila* Dot/Icm system and R64.

